RNA modifications can affect RNase H1-mediated PS-ASO activity

Katelyn A. Doxtader Lacy,[1] Xue-hai Liang,[1] Lingdi Zhang,[1] and Stanley T. Crooke[1]

[1]Core Antisense Research Ionis Pharmaceuticals, Inc, Carlsbad, CA 92008, USA

Phosphorothioate modified antisense oligonucleotides (PS-ASOs) can reduce gene expression through hybridization to target RNAs and subsequent cleavage by RNase H1. Target reduction through this mechanism is influenced by numerous features of the RNA, which modulate PS-ASO binding affinities to the RNA target, and how the PS-ASO-RNA hybrid is recognized by RNase H1 for RNA cleavage. Endogenous RNAs are frequently chemically modified, which can regulate intra- and intermolecular interactions of the RNA. The effects of PS-ASO modifications on antisense activity have been well studied; however, much less is known regarding the effects of RNA modifications on PS-ASO hybridization and RNase H1 cleavage activity. Here, we determine the effects of three different RNA modifications on PS-ASO binding and antisense activity in recombinant and cell-based systems. Some RNA modifications can reduce PS-ASO hybridization, the cleavage activity of RNase H1, or both, while other modifications had minimal effects on PS-ASO function. In addition to these direct effects, RNA modifications can also change the RNA structure, which may affect PS-ASO accessibility in a cellular context. Our results elucidate the effects of three prevalent RNA modifications on PS-ASO-mediated RNase H1 cleavage activity, and such findings will help improve PS-ASO target site selection.

INTRODUCTION

Phosphorothioate (PS)-modified antisense oligonucleotides (PS-ASOs) bind to specific RNA targets via sequence complementarity and can be designed to reduce gene expression through the cleavage action of RNase H1. Aspects of all three components of the RNA cleavage reaction contribute to the complexity of antisense activity, including (1) the RNase H1 enzyme concentration and its co-effector proteins that affect the enzymatic activity; (2) the design of the PS-ASO, which affects PS-ASO stability, RNA hybridization, and PS-ASO/protein interactions; and (3) the architecture of the target RNA, including the site of the target sequence within an RNA.[1–7] In addition, kinetic factors such as the rate of splicing, translation efficiency, the rate of degradation of the target RNA, and potential compensatory changes in target transcription or "tolerance," have all been shown to affect PS-ASO function.[8–13] These factors can affect PS-ASO activity through multiple different mechanisms, our understanding of which is continuously expanding.[14–18]

Much progress has been made in the chemistry and design of PS-ASOs to optimize activity and minimize toxicity. PS-ASOs designed to serve as substrate for RNase H1 after hybridizing to the target RNA typically consist of a central PS oligodeoxynucleotide "gap" of 8 to 12 nucleotides flanked at both ends by 2′ modified wing nucleotides.[14,19] These wing modifications include 2′-constrained ethyl (cEt), 2′-O-Methoxyethyl (MOE), 2′-O-methyl (2′OMe), and locked nucleic acids (LNA) that help improve stability against nucleases and enhance hybridization to target RNA by stabilizing an RNA-like conformation and reducing the conformational flexibility of the molecule.[20–27] Replacement of the naturally occurring phosphodiester (PO) backbone with PS increases the stability of PS-ASOs by increasing resistance to nucleases, and improves pharmacological properties through greater interactions with proteins resulting in improved tissue distribution and increased cellular uptake.[2,28–31] Recently, ASO backbone design has been further improved upon with the incorporation of the alkyl phosphonate and mesylphosphoramidate (MsPA) linkages in combination with PS, which maintains the stability and activity benefits, while modulating toxic protein-PS-ASO interactions.[32,33] In addition, position-specific ribose modifications within the gap region of the heteroduplex, such as 2′OMe at position 2 and 5′Me at positions 3 or 4, can reduce undesired cellular protein binding and mitigate toxicity.[3,34,35] Nucleobases are not often modified, as mismatches to the target RNA reduce PS-ASO hybridization; however, methylated cytosine nucleotides are used to reduce the innate immune response to PS-ASOs.[6] PS-ASO modifications, while optimizing the molecule from a pharmacological perspective, must also support RNase H1 enzymatic activity. RNase H1 makes numerous contacts with functional groups on both the RNA and PS-ASO strands that can only be achieved through a helical geometry unique to RNA/DNA hybrid duplexes.[36–38] Modifications to the PS-ASO that distort this geometry can prevent cleavage of the RNA strand.[36,37] Due to both pharmacological and biochemical restraints, PS-ASO design is constantly evolving to maximize safety and efficacy.

Features of the target RNA also significantly affect antisense activity. PS-ASO hybridization is driven primarily by the structure of the target
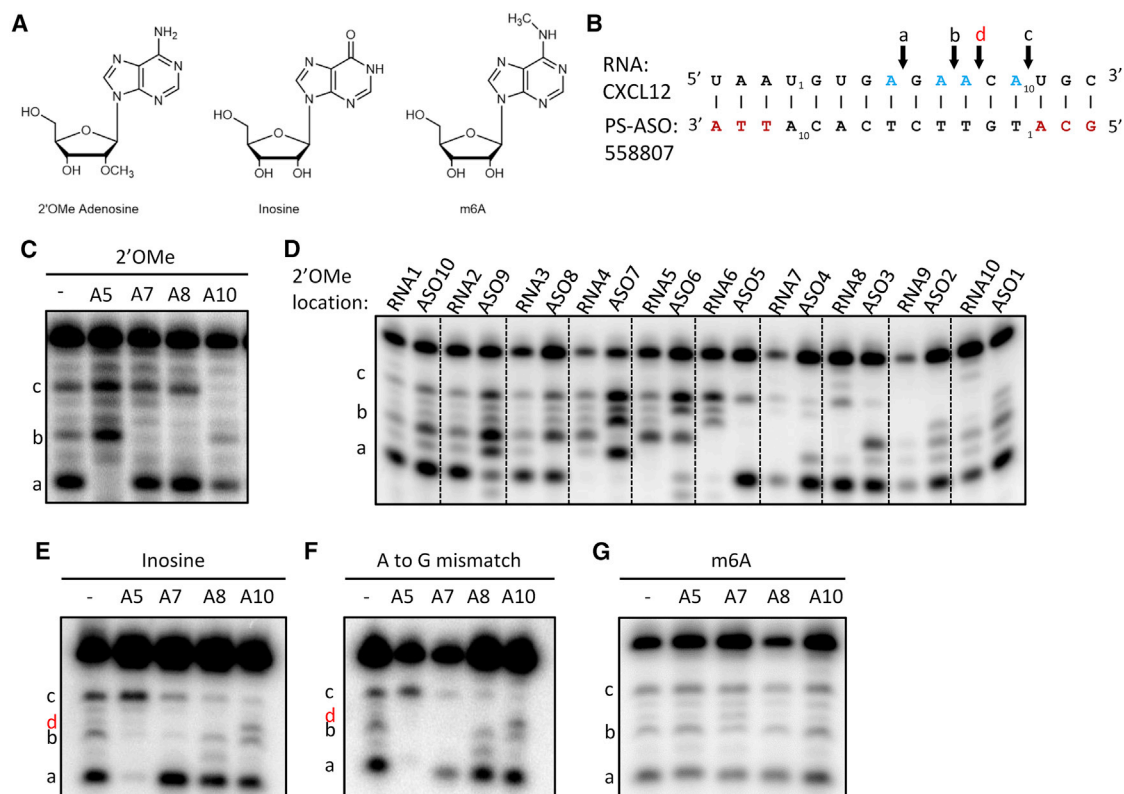
Figure 1. RNA modifications affect purified RNase H1 cleavage pattern

(A) Chemical structures of the three model RNA modifications used in this study (2′OMe tested on all four nucleobases).

(B) Schematic of the 558807/Cxcl12 PS-ASO/RNA heteroduplex used for purified RNase H1 cleavage assays. cEt modifications in the PS-ASO are indicated in red, modified nucleotides in the RNA are indicated in blue. Numbering is with respect to 5′ → 3′ for each strand. Cleavage sites "a," "b," and "c," and "d" are indicated with arrows, with cleavage site "d" highlighted in red to indicate a minor cleavage product that was increased with modifications.

(C) Cleavage pattern of 2′OMe-modified RNAs at the indicated adenosine nucleotides. Major cleavage sites are noted as "a," "b," and "c" corresponding to the positions noted in Figure 1B.

(D) Cleavage pattern of 2′OMe-modified RNA and unmodified RNA with the corresponding 2′OMe-modified PS-ASO. Numbering is with respect to the 5′ end of each strand. See also Figure 1B.

(E) Cleavage pattern of inosine-modified RNAs at the indicated nucleotides. Enhanced cleavage site induced by Ino10 noted as site "d" in red.

(F) Cleavage pattern of RNAs containing a guanosine mutation at the indicated adenosine nucleotides. Enhanced cleavage site induced by mutation at A/G10 is noted as site "d" in red.

(G) Cleavage pattern of m6A-modified RNAs at the indicated adenosine nucleotides.

RNA, and to a lesser extent, competing RNA binding proteins.[5] Recently, RNA chemical modifications have been identified as prevalent regulators of RNA maturation through modulation of RNA structure, interactions with cellular proteins, or a combination of both.[39–42] RNA modifications are found on all types of RNA, including rRNA, tRNA, small and long non-coding RNAs, and most recently, mRNA.[43,44] Biologically, chemical modification of RNA has been shown to affect RNA processing, localization, function, and stability, leading to changes in RNA splicing, export, translation, and half-life.[39,43,45] RNA modifications significantly influence gene expression and, accordingly, dysregulation of the enzymes responsible for maintaining and regulating RNA modifications is linked to various diseases and developmental disorders.[46] From the PS-ASO drug perspective, however, it remains to be understood how endogenous chemical modifications of RNA targets affect PS-ASO binding and RNase H1 cleavage. Over 150 different RNA modifications have been discovered and occur at nearly every position within the nucleotide chemical structure, on both coding and non-coding RNAs.[47] Importantly, many RNA modifications occur co-transcriptionally, suggesting that PS-ASOs are likely to encounter modified RNAs during hybridization and RNase H1 cleavage.[48–52] In order to assess how RNA modifications affect PS-ASO activity, we chose to focus on three abundant and biologically relevant RNA modifications: the 2′OMe modification on the sugar group, and the inosine and N6-methyladeosine modifications on adenosine bases (Figure 1A).

The 2′OMe modification in the ribose is commonly found in tRNAs and rRNAs as well as small nuclear RNAs (snRNAs) where it

regulates the maturation and function of these RNAs.[53–55] 2′OMe is also found in mRNAs both internally and at the 5′ cap structure of mRNAs where it modulates translation.[56,57] It has been reported that 2′OMe occurs internally in thousands of mRNAs, with average of 1.4 sites per methylated mRNA.[58] This modification can be deposited directly by specific methyltransferases or through the action of guide small nucleolar RNAs (snoRNAs) and the methyltransferase fibrillarin.[59–61] As the 2′OH group of RNA is responsible for both its sensitivity to degradation and its flexibility to adopt unique 3D structures, methylation of this position accordingly affects the RNA's stability and structure.[26,42]

RNA structure and processing can also be regulated through modification of adenosine bases. Deamination of adenosines to the "fifth" nucleotide—inosine—is catalyzed by the ADAR enzymes and commonly referred to as "RNA editing." Genome-wide analysis identified millions of A-to-I editing events in RNA from human tissues, with as many as 85% of mRNAs containing inosine.[49,62,63] Humans possess three ADAR genes; however, only ADAR1 and ADAR2 are catalytically active.[64,65] ADARs do not have a strong sequence preference for modification, but require double-stranded RNA as a substrate.[66] Deamination disrupts Watson-Crick base pairing and destabilizes structured RNA,[67,68] which has been shown to regulate the innate immune response and the RNA interference pathways.[69,70] RNA editing can also result in protein coding changes, modulate translation by altering the stop codon, or direct alternative splicing through mutations of splice sites.[71,72] Furthermore, ADARs can regulate the localization of some RNAs and modulate protein-RNA interactions in an editing independent manner.[73]

N6 methyladenosine is another common modification of adenosines, and the most common modification found in mRNAs, with one to three m6A modifications per transcript.[74,75] Unlike inosine, this modification is deposited by specific methyltransferases through recognition of consensus sequences.[74–76] M6A modification of RNA can affect RNA structure similarly to inosine by weakening Watson-Crick base pairing, and destabilizing double-stranded RNA (dsRNA).[77–81] This in turn can affect how the RNA interacts with cellular proteins.[40,41] Primarily, however, the m6A modification effects are through the action of reader proteins, which bind to the modified nucleotide and alter the RNA's fate or function.[82]

Given the prevalence of RNA modifications and their effects on RNA structure and processing, it is important to understand how they might affect PS-ASO activity. Here we describe the effects of three RNA modifications on PS-ASO-mediated RNase H1 activity. The 2′OMe modification protects 2′OH groups from the nuclease in the RNA strand and can inhibit RNase H1 cleavage at the adjacent 5′ and 3′ sites of the modified nucleotide, thereby slowing the extent of RNase H1 cleavage over time. In contrast, the inosine modification can block cleavage at the modified nucleotide as well as distal from the modified site, and can also enhance cleavage at minor sites within the gap. M6A modification of RNA does not directly affect the cleavage pattern of RNase H1, nor does it alter cleavage patterns via RNA struc-

tural changes when the m6A modification is placed within in a model stem-loop RNA. While we observed clear effects of RNA modifications on RNase H1 cleavage activity in test tubes, the effects in cells were more subtle for the tested RNA targets. These observations will help PS-ASO target site selection by knowing which RNA modifications may affect PS-ASO interactions with the target sequence and alter RNase H1 enzymatic activity, and which modifications can be more tolerated, better facilitating the identification of lead PS-ASOs.

RESULTS

RNA modifications can alter the cleavage pattern of RNase H1

RNase H1 requires specific features of the RNA/DNA hybrid for effective RNA cleavage to be mediated by the enzyme. The catalytic domain of RNase H1 contacts two 2′OH groups on either side of the scissile phosphate, requiring a total of four consecutive RNA nucleotides.[83] On the DNA side, RNase H1 binds via a contorted phosphate binding pocket and a DNA binding channel, which can only be achieved by adopting the unique B form geometry specific to RNA/DNA hybrids.[83] RNA ribose modifications, such as 2′OMe, would likely affect duplex recognition by RNase H1 by clashing with the 2′ binding interface, whereas RNA base modifications such as m6A and A-to-I editing may affect the helical geometry of the duplex or potentially hybridization with the PS-ASO. Thus, we used these three abundant modifications as models to interrogate how RNase H1 cleavage and PS-ASO activity could be altered by RNA modifications (Figure 1A).

To determine the direct effects of RNA modifications on RNase H1 cleavage, we used a well-characterized 3-10-3 cEt gapmer PS-ASO (Ionis #558807) with its complementary, size-matched RNA, derived from the mouse *Cxcl12* gene, modified at various positions in the region hybridized with the gap region of the PS-ASO (Figures 1B and S1A).[33,35] Assessing the cleavage pattern at a single time point showed that both RNA ribose and base modifications could change the cleavage pattern, i.e., where in the RNA strand RNase H1 cut (Figure 1C). The 2′OMe modification prevented RNase H1 cleavage on both the 5′ and 3′ sides of the modified nucleotide, as evidenced by the abolished cleavage at site "b" by 2′OMe at positions A7 and A8 of the RNA (Figure 1C). 2′OMe modification appeared to have limited effect on RNase H1 cleavage sites that were not adjacent to the modified nucleotide. Expanding this analysis to each nucleotide in the gap further confirmed that 2′OMe can affect cleavage at adjacent nucleotides both upstream and downstream of the modified position (Figure 1D). RNA that was 2′OMe modified at RNA positions 1 to 3 did not have an altered cleavage pattern, whereas introduction of 2′OMe at RNA positions 4 to 10 did change where RNase H1 was able to cleave. This is consistent with previous findings that RNase H1 binds the heteroduplex at the 5′RNA/3′DNA end and cleaves the RNA 7 to 10 nucleotides downstream.[36]

Next, we compared the effects of the 2′OMe modification on cleavage patterns when the modified nucleotides are placed in the RNA strand or in the PS-ASO strand at the corresponding position. While some cleavage patterns were similar between 2′OMe-modified RNAs and

unmodified RNAs with the corresponding 2′OMe-modified PS-ASOs, at several positions, the 2′OMe modification produced different cleavage patterns depending on which strand it was placed (Figure 1D). When placed in the PS-ASO strand, the 2′OMe modification blocked cleavage only at RNA adjacent nucleotides downstream from the modified position, unlike the 2′OMe-modified RNA, which prevented cleavage both upstream and downstream from the modification (compare RNA6/ASO5). Moreover, 2′OMe-modified PS-ASOs alter RNA cleavage at non-adjacent sites farther downstream from the modified nucleotide, for example, 2′OMe at ASO4 reduces cleavage at site "c." Last, in a few cases (ASO7 and ASO 9), introduction of 2′OMe on the PS-ASO results in enhanced RNA cleavage at minor sites relative to the pattern of the unmodified RNA/PS-ASO. The differences in cleavage pattern between 2′OMe-modified RNAs and unmodified RNA with 2′OMe-modified PS-ASOs highlights the specific requirements of RNase H1 for each strand of the hybrid duplex.

The 2′OMe modification has been used in PS-ASOs to improve hybridization with RNA, with approximately 0.5°C Tm increase per 2′OMe modification,[84] so we asked whether the same was true for 2′OMe-modified RNA. When placed in the target RNA, the 2′OMe modification had a negligible effect on duplex thermal stability (Figure S1B). These data suggest that 2′OMe effects on RNase H1 cleavage pattern are not due to altered hybridization of the PS-ASO to the target RNA, but more likely are through disruption of the RNA ribose moieties recognized by RNase H1.

RNA base modifications are likely to have different effects on PS-ASO function as compared with ribose modifications, and, indeed, the effects of the inosine modification at the same sites within the Cxcl12 RNA are distinct from the effects of the 2′OMe modification. Introduction of inosine significantly reduced RNase H1 cleavage at the modified site, without completely ablating cleavage (Figure 1E). Inosine modification also affected non-adjacent RNase H1 cleavage sites primarily in the 3′ direction from the modified site. In the case of Inosine A10, enhanced cleavage of a minor cleavage site was observed (site "d") while the cleavage at site "c" observed with the parent RNA was reduced. Mutation of the Ade to Gua in the RNA, creating a mismatch in the duplex, produced an identical cleavage pattern to the inosine-modified RNA (Figure 1F), consistent with the fact that inosine mimics guanosine. Moreover, the thermal stability of the RNA/PS-ASO duplex was noticeably reduced by inosine modification, similarly to an A:G-mutated RNA, though not below the reaction temperature, allowing cleavage activity to be maintained (Figure S1C). As it is known to do in dsRNA, we observed inosine perturbing the local hybridization of the RNA and PS-ASO.[67,68] This perturbation may, in turn, alter the overall geometry of the RNA:DNA duplex, which could enable inosine modifications to affect RNase H1 cleavage distal from the modified site, while not completely blocking cleavage at the native sites.

Importantly, not all RNA base modifications affect PS-ASO function. Unlike inosine, the m6A base modification did not affect the RNase H1 cleavage pattern at any tested position (Figure 1G). This is consistent with the m6A modification's ability to maintain base pairing, though a suboptimal conformation is adopted.[78] This suboptimal base pairing is reflected by the modestly reduced T_m of m6A-modified RNAs hybridized with PS-ASOs (Figure S1D). Our data demonstrate that some RNA modifications can modulate PS-ASO hybridization, and change where RNase H1 can cleave the target RNA, whereas other RNA modifications can be tolerated by RNase H1 and leave cleavage patterns unaltered.

RNA modifications can affect RNase H1 cleavage activity
Next, we examined how RNase H1 cleavage activity over time could be affected by RNA modifications. We determined the enzymatic activity over time as a fraction of total cleavage products generated relative to the total input (Figures 2A–2C, Materials and methods). In general, modified RNAs were cleaved to a lesser extent over time by RNase H1 compared with the unmodified RNA substrate, demonstrating that RNA modifications change the kinetic parameters of RNase H1 cleavage activity (Figures 2A–2C). Moreover, these results suggest that the loss of certain cleavage sites due to the RNA modification cannot be entirely recouped by RNase H1 cleaving at alternative sites (Figures 2A, 2B, and 1C–1E). While the m6A modification did not affect the cleavage pattern, it modestly reduced the extent of cleavage over time by RNase H1 (Figure 2C). It is possible that the m6A modification alters the geometry of the duplex such that RNase H1 cleavage is suboptimal, but does not alter the duplex enough such that RNase H1 cleavage is shifted or lost entirely.

The m6A modification has a well-characterized role in modulating RNA structure, suggesting an alternative mechanism by which this modification could affect PS-ASO activity.[40] We synthesized an RNA with a hairpin structure derived from the *MAT2A* RNA 3′UTR, known to contain an m6A modification in its terminal loop region, and tested different PS-ASOs that placed the m6A at different positions within the RNA/PS-ASO heteroduplex (Figure S2A and Tables S1 and S2).[76,85] No changes in the RNase H1 cleavage pattern were observed with any of the PS-ASOs between the modified and unmodified RNA substrates (Figure S2B). Last, we attempted to test the activity of PS-ASOs targeting the hairpin in cells after siRNA reduction of *METTL16* , the methyltransferase responsible for the m6A modification of the hairpin.[76] Unfortunately, there was no activity for the PS-ASOs tested, in the presence or absence of the methyltransferase, suggesting that this region of the RNA is inaccessible to PS-ASO binding in cells, potentially due to protein binding or RNA structure (data not shown). Taken together with the modest effects of the m6A modification on RNase H1 cleavage in our test tube studies, and the challenge of testing the effects of the m6A modification on PS-ASO activity in cells, the inosine and 2′OMe modifications were further evaluated in subsequent studies.

2′OMe modifications mildly affect PS-ASO activity in cells
Our studies with PS-ASO 558807 and its size-matched complementary RNA demonstrated that RNase H1 cleavage was altered in both location and extent over time by the presence of 2′OMe in the
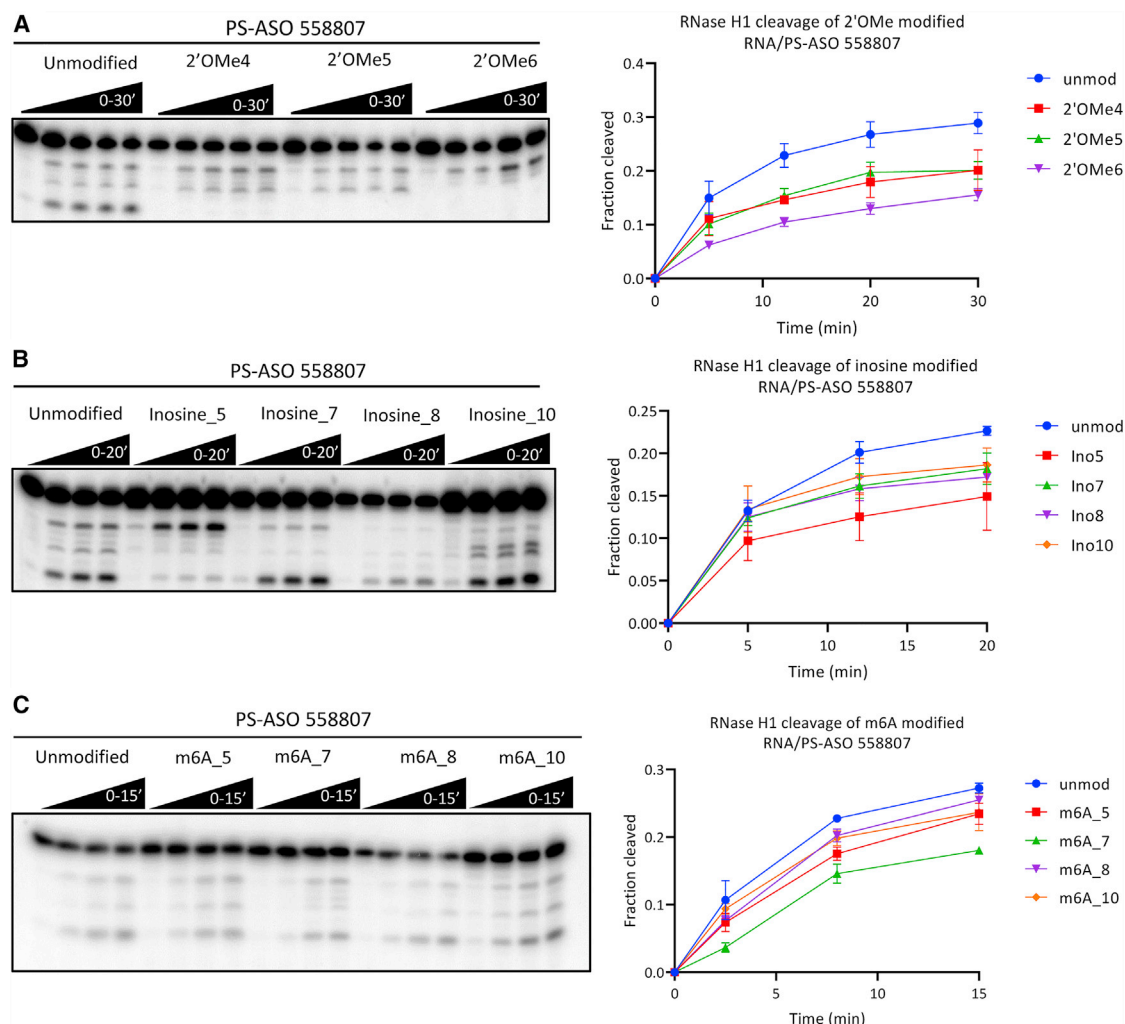
Figure 2. RNA modifications reduce purified RNase H1 cleavage extent over time

(A–C) Extent of cleavage over time of modified RNAs duplexed with PS-ASO 558807. Curves show fraction of all cleavage products relative to the total signal in each lane. Data points represent the average of three replicates and error bars indicate the standard deviation.

heteroduplex region. Cellular target RNAs, however, have long flanking sequences, are often structured, and are commonly bound by proteins. These features could influence the effects of the 2′OMe modification on PS-ASO-mediated RNase H1 activity. Thus we sought to test PS-ASO activity in a cell-based context on a naturally occurring 2′OMe-modified target. We chose the U6 snRNA as our model RNA target because we could modulate a specific 2′OMe modification at Ade53 by reduction of the guide snoRNA, *SNORD8*, known to be responsible for its deposition.[86] Using a gapmer PS-ASO targeting *SNORD8*, we could significantly reduce the snoRNA level in cells as compared with treatment with a size- and chemistry-matched control PS-ASO (Figure 3A). Importantly, reduction of *SNORD8* did not affect U6 snRNA abundance or processing, since the level and size of U6 snRNA were essentially unaltered (Figure 3A). In addition, we did not observe global effects on splicing upon *SNORD8* reduction under the experimental conditions, as deter-

mined using the qPCR assay for the levels of several mRNAs and the corresponding pre-mRNAs (Figure S3A).

To detect the presence of 2′OMe at Ade53 in the U6 snRNA we used reverse transcription primer extension assays using different concentrations of deoxyribonucleotide triphosphate (dNTP).[87] In cells treated with the control PS-ASO, we observed the 2′OMe modification of U6 at Ade53 as evidenced by primer extension stops in the low dNTP condition and readthrough of the same region in the high dNTP condition (Figures 3B and S3B). After treatment with the *SNORD8* PS-ASO, we observed a 50% reduction in primer extension stops at Ade53 under low dNTP conditions, indicating a reduction in the presence of the 2′OMe at this position, while the 2′OMe modification at Ade47 was unaffected (Figure 3B). This modest reduction of 2′OMe level is likely due to the relatively long half-life of the U6 snRNA (~24 h).[88]
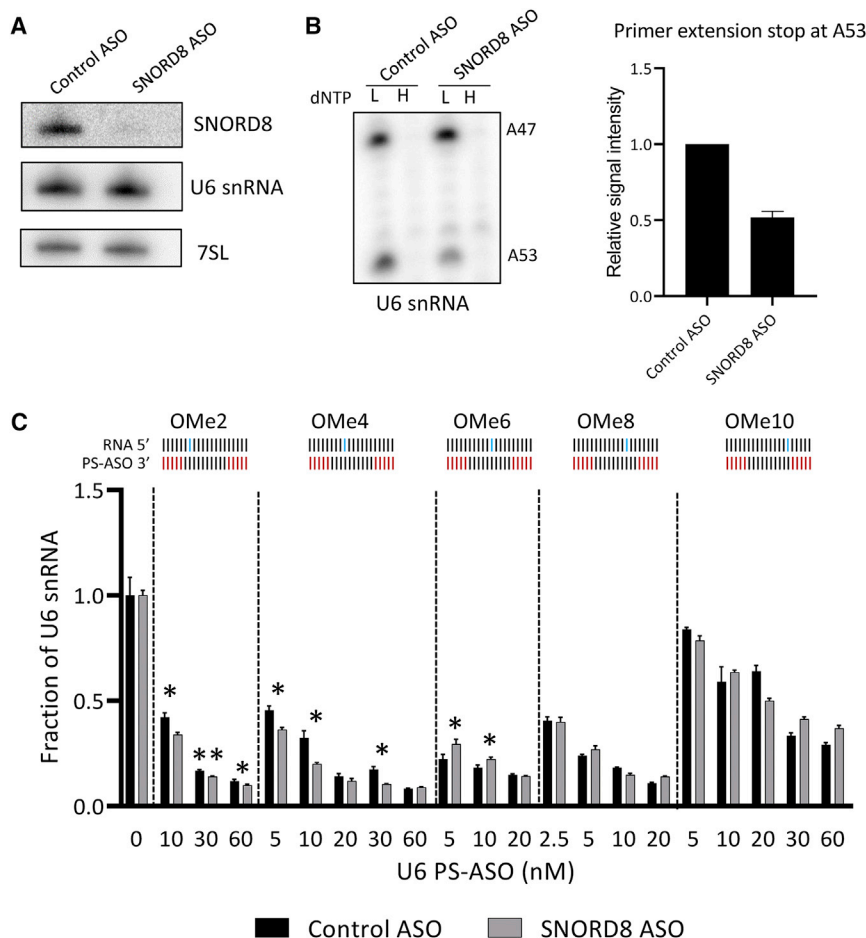
Figure 3. The 2′OMe modification in the U6 snRNA has minimal effect on cellular PS-ASO activity

(A) Northern blot analysis of *SNORD8* and the U6 snRNA after treatment of 293FT cells with control or *SNORD8* PS-ASO; 7SL RNA is shown for normalization.

(B) Primer extension analysis of the U6 snRNA after reduction of *SNORD8*. "L-low" is 0.02 mM dNTP and "H-high" is 5 mM dNTPs. The 2′OMe modifications in the U6 snRNA at A47 and A53 are indicated by primer extension stops in the "low-L" dNTP lanes, which are absent in the "high-H" dNTP lanes. Quantification of the primer extension stop band is shown on the right, expressed as an average of three replicates with error bars representing the SD.

(C) Activity of PS-ASOs targeting the U6 snRNA placing the 2′OMe modification at the different positions within the heteroduplex gap region. Labels and blue lines in the top strand indicate where within the RNA the 2′OMe modification is relative to the heteroduplex formed by PS-ASO hybridization (bottom strand). Red lines in the PS-ASO strand indicate MOE modifications. Data represented as an average of three replicates, with error bars showing the SD. Asterisks represent p values derived from t tests comparing the control and *SNORD8* reduced samples at each concentration of PS-ASO. *p < 0.05, **p < 0.01.

Next, we assessed the antisense activity of five U6-targeting PS-ASOs (Table S1), which hybridized such that Ade53 was placed at different positions within the heteroduplex, and compared the activity between control (methylated) and *SNORD8* reduced (less methylated) cells. The reduction of the Ade53 methylation of U6 slightly increased PS-ASO activity when the 2′OMe modification in the RNA was at position 2 or 4 within the heteroduplex, compared with no change in activity when the Ade53 modification was placed in position 8 of the gap region (Figure 3C). However, when the 2′OMe is at position 6 or 10, we observed slightly decreased activity upon methylation reduction and no significant difference in activity with the 2′OMe modification at position 8 within the RNA. Overall, the effects of 2′OMe on cellular ASO activity are very minor, demonstrating that although 2′OMe disrupts recombinant RNase H1 cleavage and reduces cleavage extent over time, the effect of 2′OMe on ASO activity in cells can be modest.

Inosine modifications mildly affect PS-ASO activity in cells

As with the 2′OMe modification, PS-ASOs encounter inosine modifications in the context of structured RNA and cellular proteins, thus we tested the effects of inosine modifications on PS-ASO activity in cells. It has been reported that the mRNA of a

DNA replication complex component, *GINS1*, is edited within its 3′UTR.[89] The inosine modification is recognized as a Gua base by polymerases, thus the detection of inosine is straightforward via RT-PCR followed by Sanger sequencing, in which the edited sites will present as a mixture of Ade and Gua bases. To confirm the reported A-to-I editing event, cDNA was synthesized from a portion of the *GINS1* 3′UTR, amplified by PCR, and subjected to sequencing analysis. Indeed, we observed A-to-I editing at A2623 and A2699 within the *GINS1* 3′UTR (Figure 4A top, Table S3). We synthesized size-matched RNAs from both regions containing the inosine at the endogenous positions, placing the modified nucleotide at position 6 (RNA1 for region 1) or position 4 (RNA 2 for region 2) within the heteroduplex, and tested the cleavage patterns with the corresponding PS-ASOs to recapitulate our experiments with the 558807 PS-ASO and the *Cxcl12* RNA. In three separate sequence contexts (*Cxcl12* and *GINS1* RNA1 and RNA2), we observed changes in RNA cleavage pattern by RNase H1 due to the presence of inosine (Figures 4B, S4A, S4B, and 1E). Interestingly, in the *GINS1* RNA2 sequence, the addition of the inosine modification completely ablated certain cleavage products instead of merely reducing them (site "b"). We also observed enhanced cleavage at a minor cleavage site in RNA2 3′ relative to the inosine modification similar to what we observed in the *Cxcl12* sequence, but also 5′ relative to the inosine modification in RNA1 (site "a") (Figures 4B, S4A, S4B, and 1E). These subtle differences in the effects of the inosine modification on cleavage pattern highlight the importance of sequence context
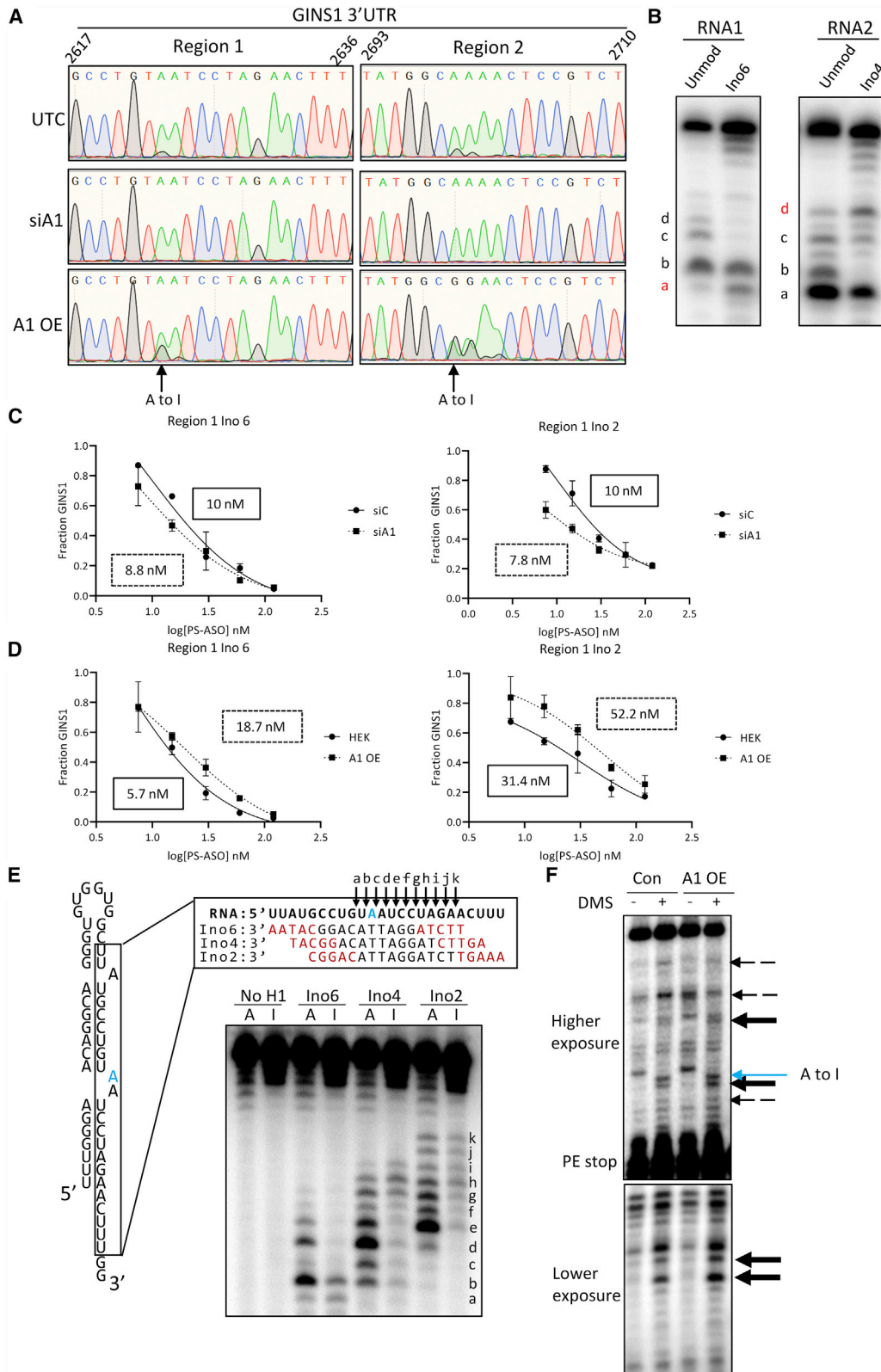
(legend on next page)

when evaluating PS-ASO-guided RNase H1 cleavage. Regardless, our observations that inosine can affect the cleavage pattern of RNase H1 remain true in different sequence contexts.

Analyzing the effects of reduction of the two catalytically active deaminases, ADAR1 and ADAR2, showed that ADAR1 was the responsible enzyme for editing these sites within *GINS1* (Figure 4A middle and S4C, ADAR2 data not shown). We also established a stable cell line overexpressing the p150 isoform of ADAR1, which allows us to survey the effects of editing on antisense activity in both the nucleus and the cytoplasm.[11,90] Overexpression of ADAR1 noticeably increased the Gua signal in the sequencing results at the same sites within both regions, indicative of increased A-to-I editing (Figure 4A bottom and S4C). Using this system in which we could increase and decrease the presence of inosine at a given site, we measured the activity of PS-ASOs targeting both edited regions of *GINS1*. Reduction of ADAR1 and consequent decrease in inosine modification resulted in a slight increase in the potency of PS-ASOs targeting both regions (Figure 4C and S4D). Accordingly, ADAR1 overexpression could slightly reduce the activity of the same PS-ASOs (Figures 4D and S4E). While these observations are consistent with what was observed in test tubes, the overall effects for this target in cells are not significant when compared with the variation in activity of PS-ASOs targeting unedited control genes such as *nucleolin* (NCL) (Figure S4F). These results suggest that in this sequence context, RNase H1 can overcome inosine-induced changes in the heteroduplex in cells.

A-to-I editing may affect RNA structure in a fashion that can modulate RNase H1 cleavage

While our results thus far suggest a direct effect on RNase H1 cleavage due to RNA modifications within the heteroduplex, it is also possible that RNA modifications outside of the heteroduplex region could induce structural changes in the RNA and affect PS-ASO activity. To determine the specific mechanisms for how inosine modification of *GINS1* reduces RNase H1 cleavage, we synthesized a 52nt RNA fragment derived from *GINS1* Region 1 containing unmodified adenosine, or edited to inosine at the verified position, within a stem-loop structure (Figures 4E and Table S2). We assessed the cleavage patterns of three PS-ASOs, which hybridized such that the inosine modifica-

tion was at positions 6, 4, and 2 within the gap (Table S1). Consistent with the size-matched data, we found that A-to-I editing in a longer RNA context also affected the cleavage patterns of the three PS-ASOs tested (Figure 4E). The inosine modification reduced cleavage mediated by PS-ASO Ino6 at sites adjacent to (site "b") and 3′ distal from (sites "d" and "e") the modified nucleotide, while slightly enhancing cleavage at a site 5′ relative to the inosine nucleotide (site "a"). After shifting the position of the inosine nucleotide within the heteroduplex by using PS-ASO Ino4 or Ino2, we also observed reduced cleavage relative to unmodified RNA at sites adjacent to the inosine nucleotide, and at sites extending 3′ from the modified nucleotide. However, cleavage sites five or more nucleotides away from the inosine nucleotide were unaffected (sites "g" and "h" for RNA cleavage with Ino4 and sites "h" through "k" for RNA cleavage with Ino2). We observed similar effects on cleavage in the structured context of *GINS1* Region 2 RNA (Figure S5A). Importantly, this shows that inosine can directly affect RNase H1 cleavage while in the naturally occurring structured RNA context, where inosine modifications are commonly found.[66] The general trends of altered RNase H1 cleavage observed with the length-matched RNA/PS-ASO duplex were consistent in the stem-loop RNA studies. The presence of inosine prevented RNase H1 cleavage at various positions upstream and downstream from the modified site as well as enhanced minor cleavage sites for RNase H1 (Figures 4E and S5A).

Inosine modifications are known to influence RNA structure.[67,68] Dimethyl sulfate (DMS) treatment modifies accessible Ade and Cyt nucleotides, leading to DMS-dependent primer extension stops, indicating unpaired regions of the RNA. We treated control and ADAR1 overexpressing cells with and without DMS, and performed primer extension analysis to survey the edited region 1 of the *GINS1* mRNA for changes in solvent accessibility (Figure S5B). Indeed, we observed differences in the DMS-dependent primer extension stops in the *GINS1* mRNA from ADAR1-overexpressing cells, relative to control cells, and due to a strong, DMS-independent, primer extension stop, we present the gel at two different exposures (Figures 4F and S5B). Relative to control cells, some nucleotides in ADAR1-overexpressing cells become more accessible to DMS modification as represented by a stronger primer extension stop band (thicker arrows),

---

Figure 4. Inosine can mildly affect PS-ASO activity in cells and RNA structure

(A) RT-PCR followed by Sanger sequencing of a portion (nt 2617–2710) of the *GINS1* 3′UTR in control cells, ADAR1-reduced, or ADAR1-overexpressing cells (see also Table S3 and Figure S4C). A-to-I editing can be detected by the mixture of Ade (green) and Gua (black) signals also indicated with an arrow.

(B) Cleavage pattern of size-matched RNAs from the two edited regions of the *GINS1* 3′UTR with or without inosine modifications at the indicated positions. Cleavage sites a–d are indicated, those in red indicate cleavage sites that are enhanced with inosine modification of the RNA. See also Figure S4B for more detailed information.

(C) *GINS1* Region 1 PS-ASO activity in control or ADAR1-reduced cells. Data represented as an average of four replicates, with error bars showing the SD. Solid boxed number is the IC50 of the PS-ASO in control cells, and dashed boxed number is the IC50 of the PS-ASO in ADAR1 reduced cells.

(D) *GINS1* Region 1 PS-ASO activity in control or ADAR1 overexpressing cells. Data represented as an average of four replicates, with error bars showing the SD. Solid boxed number is the IC50 of the PS-ASO in control cells, and dashed boxed number is the IC50 of the PS-ASO in ADAR1 overexpressing cells.

(E) Cleavage pattern of *GINS1* Region 1 stem-loop RNAs with or without inosine with different PS-ASOs placing the modified nucleotide at the indicated position. Schematic of the stem loop indicating the position of inosine (in the RNA strand) within the stem loop and the tested PS-ASOs is on the left. Lowercase letter labels indicate the cleavage site within the RNA.

(F) DMS footprinting of *GINS1* Region 1 in control and ADAR1 overexpressing cells. The data are from the same gel shown at different exposures due to the strong, DMS-independent primer extension stop labeled on the left. Dashed/bold arrows designate reduced/increased primer extension stops in the ADAR1 overexpressing cells relative to control, indicating increased/decreased accessibility, respectively. The A-to-I modified nucleotide is also indicated with a blue arrow. See also Figure S5B.

whereas some other nucleotides are less accessible as represented by a weaker band (dashed arrows). This indicates there are alterations in the RNA structure in ADAR1-overexpressing cells, which is likely due to the increased A-to-I editing we observe in this region (Figures 4A and 4F). We hypothesized that these inosine-induced structural changes could affect PS-ASO activity at sites distal from the modified nucleotide. We next used the stem-loop RNAs with and without inosine and tested nine PS-ASOs that bound upstream of the modified nucleotide spanning the stem-loop structure (Figure S5C and Table S1). None of the PS-ASOs appeared to have an altered cleavage pattern with the inosine-modified RNA, as compared with the unmodified RNA counterpart (Figure S5C). It is possible that the local structure of this region is different in the context of the entire transcript and cellular proteins in cells, compared with our arbitrarily selected portion of the RNA used for test tube studies. However, when we tested the activity of two of the same PS-ASOs that bound upstream of the modified nucleotide in cells, we saw little change in the activity in cells (Figure S5D). These results suggest that although inosine can modulate RNA structure, a single inosine modification in this sequence context is not enough to significantly affect PS-ASO activity.

DISCUSSION

PS-ASO-mediated RNA cleavage by RNase H1 is influenced by numerous factors. To optimize PS-ASO activity, a detailed understanding of the features of endogenous RNA targets is required. In this study we determined how several prevalent RNA modifications influence PS-ASO activity. We showed that ribose modifications such as 2′OMe alter the cleavage pattern of RNase H1 and reduce the extent of cleavage over time, without deleterious effects on the stability of the RNA:PS-ASO hybrid. The cleavage patterns of the 2′OMe-modified RNAs are distinct from the cleavage patterns of unmodified RNA with 2′OMe-modified PS-ASOs at the analogous positions. In cells, however, the 2′OMe modification on RNA has little to no effect on PS-ASO activity. Modifications to the RNA bases such as inosine can affect the thermal stability of the heteroduplex and alter RNase H1 cleavage pattern and extent over time, potentially through modifying heteroduplex geometry. In cells, however, the effects of the inosine modification are also minor, but are consistently negatively correlated with PS-ASO activity when the inosine nucleotide is within the heteroduplex. In addition, we tested how inosine induced RNA structural changes in the *GINS1* 3′UTR sequence context influence how well PS-ASOs mediate target cleavage, and also found the effects to be minor. Importantly, some functional RNA modifications do not affect the PS-ASO cleavage pattern, as is the case for the m6A modification. Understanding which RNA modifications are more or less tolerated by PS-ASO-mediated RNase H1 cleavage will help improve PS-ASO design and target site identification.

Chemical modification of RNA mediates intra- and intermolecular hybridization, as well as interactions with RNA binding proteins. Introduction of the 2′OMe modification on the target RNA prevented RNase H1 cleavage at the modified site; however, these single modifications did not reduce the thermal stability of the hybrid

significantly, and even subtly increased overall stability when introduced at some positions. Altered hybridization due to 2′OMe modification is unlikely to be the mechanism through which this modification modulates RNase H1 cleavage. However, it is likely that if the 2′OMe modification is found adjacent to additional RNA modifications, as is common in non-coding RNAs, the 2′OMe modification could significantly increase the stability of RNA structure, reducing PS-ASO binding and dramatically limit RNase H1 cleavage, rendering the target site less accessible for PS-ASOs. Interestingly, this could potentially explain why the PS-ASO targeting U6, which places Ade53 at position 10, is less active than the other PS-ASOs in this region, as this PS-ASO also places an additional 2′OMe modification (A47) at position 4 within the gap region of the heteroduplex (Figures 3B and 3C).

Previous structural and biochemical work suggests why 2′OMe modifications of the RNA disrupt cleavage. RNase H1 requires four consecutive 2′OH groups with which it contacts via backbone and side chain interactions within its catalytic domain.[83] While 2′ modifications have been shown previously not to affect RNase H1 binding affinity to the duplex, addition of the methyl group at the 2′ position of the ribose would disrupt this series of interactions and require RNase H1 to traverse the hybrid to establish the necessary contacts for cleavage.[91] This alone does not suggest that overall cleavage should be reduced if RNase H1 is able to compensate by cleaving at alternative positions within the hybrid; however, in the case of the PS-ASO 558807 and its size-matched target RNA from the *Cxcl12* gene, we do observe reduced cleavage over time. This could be because RNase H1 requires a minimum length of 7 to 10 RNA:DNA hybridized nucleotides to bind with its hybrid binding domain and cleave the RNA downstream.[36] Limiting the sites RNase H1 can cut with 2′OMe modifications within the fixed hybrid length determined by the PS-ASO could explain why the overall cleavage extent over time is reduced in our cleavage studies. In addition, this length requirement and the positioning of RNase H1 on the heteroduplex explains why we see positional effects of the 2′OMe modification on RNase H1 cleavage. In the Cxcl12 sequence targeted by PS-ASO 558807, 2′OMe modifications at positions 1 to 3 of the RNA target had no effect on cleavage pattern, as these positions are within seven nucleotides from the start of the RNA:PS-ASO hybrid, and where the hybrid binding domain of RNase H1 should bind.[36] On the other hand, RNAs modified farther downstream from the start of the hybrid, at positions 4 to 10, do have altered cleavage patterns relative to unmodified RNA. These cleavage patterns influenced by the positions of 2′OMe support previous work that showed that the hybrid binding domain of RNase H1 binds the 5′RNA/3′ASO end of the duplex and the catalytic domain cuts the RNA downstream.[36]

RNase H1 can bind dsRNA (albeit with lower affinity than RNA/DNA hybrids) but its cleavage activity is optimal to the RNA strand within heteroduplexes.[92] While RNase H1 recognizes the sugar-phosphate backbone of the RNA for sequence independent cleavage, it also requires a specific duplex geometry adopted by RNA:DNA hybrids

for productive catalysis.[83] The different cleavage patterns we observe for the 2'OMe-modified RNAs and unmodified RNA with corresponding 2'OMe-modified PS-ASOs are therefore predictable from the structural data. The bidirectional effects of the 2'OMe modification on RNA are consistent with disruption of the interaction network made between the catalytic domain of RNase H1 and the 2'OH groups of unmodified RNA; addition of a methyl group would destabilize contacts with active site residue E186.[83] On the other side of the duplex, the addition of a 2'OMe to the DNA/PS-ASO would not directly disrupt protein-ASO contacts; however, 2' modifications that stabilize the C-3'*endo* sugar conformation of PS-ASOs prevent recognition of the DNA strand via the phosphate binding pocket of RNase H1.[83] The structural requirements of RNase H1 explain the altered cleavage patterns we observe, and how the cleavage patterns of 2'OMe-modified PS-ASOs are distinct from 2'OMe-modified RNAs.

While our test tube studies make a strong case for the 2'OMe modification affecting PS-ASO activity, our cell-based data show a less robust phenotype. The 2'OMe modification in the context of the U6 snRNA had limited effects on PS-ASO activity. This is likely because the reduction of the 2'OMe modification at Ade53 through knockdown of the guide snoRNA was only 50%, presumably due to slow turnover of the U6 snRNA.[88] This is also consistent with previous observations that knockdown of METTL16, the responsible enzyme for m6A modification of U6, did not substantially reduce the m6A level on U6 RNA.[76] An additional explanation is that both 2'OMe modification and PS-ASO-mediated cleavage can occur co-transcriptionally; therefore, it is possible that the cleavage happens faster than the modification, leading to little change in target reduction.[52,93] It is also possible that in other targets (sequence contexts) the 2'OMe modification could be more detrimental to PS-ASO-mediated cleavage of RNA in cells. Despite the minor effects we observe on U6 PS-ASO activity in cells, our understanding of how RNase H1 interacts with the target RNA and our biochemical data showing reduced cleavage extent over time with 2'OMe-modified RNA substrates indicate that the 2'OMe-modified region in RNA should be avoided in PS-ASO target selection, especially in the gap region.

Inosine-modified RNAs are also cleaved less efficiently than unmodified RNAs by purified RNase H1. Inosine is interpreted by the cell as a guanosine, and accordingly, inosine pairs with uracil (and presumably with thymidine as well) less stably than adenosine.[67] Therefore, the similarity of the cleavage patterns and thermal stability of A-to-I- or A-to-G-modified RNAs is expected. This presents a unique challenge in PS-ASO design, as a PS-ASO designed to hybridize to the sequence of the target would be encountering an inosine-modified RNA as if it were a mismatched target. Previously, it has been shown that while RNase H1 can accommodate some mismatches in the heteroduplex, as is obvious from this study as well, PS-ASO activity is reduced relative to the perfectly matched target sequence.[5] Despite a minor effect of inosine on PS-ASO modification in cells, our data indicate that inosine-modified sites should also be avoided during ASO target selection.

While both modifications ultimately reduce RNase H1 cleavage in test tubes, the cleavage pattern of 2'OMe-modified RNAs is distinct from the cleavage pattern of inosine-modified RNAs at the same positions, suggesting that these modifications affect RNase H1 cleavage differently. Inosine modifications are not likely to disrupt direct contacts with RNase H1, rather, the alternate hydrogen bonding network formed between inosine and thymidine could result in distortions of the geometry of the heteroduplex. This could lead to suboptimal binding by RNase H1 to the heteroduplex, inefficient cleavage of a contorted active site, or a combination of both, manifesting in reduced cleavage over time in both recombinant and cell-based contexts. Importantly, we observe these effects in multiple sequence contexts with the inosine placed at different positions within the gap, suggesting that inosine should generally be avoided in PS-ASO target selection.

In addition to the direct effects of inosine on RNase H1 cleavage when it is placed within the heteroduplex, inosine modifications can alter RNA structure, which is known to affect PS-ASO activity.[5] While inosine destabilizes dsRNA, it is also known to stabilize single-stranded/dsRNA junctions.[68] We detected structural changes of the *GINS1* Region 1 RNA upon ADAR1 overexpression; however, we did not observe a corresponding change in PS-ASO activity. In other RNA targets, however, structural changes could lead to altered accessibility for PS-ASOs targeting the editing complementary sequence, or potentially even farther distal sites from the modified nucleotide. Moreover, it is also possible that inosine modifications (and/or the structural changes they induce) can lead to differential protein binding to edited regions, further complicating PS-ASO accessibility and activity.

The most prevalent mRNA modification, m6A, does not affect RNase H1 cleavage pattern in our purified system, for either the *Cxcl12* sequence targeted by PS-ASO 558807, or a canonical m6A-modified RNA stem-loop target. The m6A modification mildly reduces PS-ASO hybridization to RNA; however, any distortions to the duplex that may occur due to altered hybridization do not affect where RNase H1 cleaves the RNA. Nevertheless, since m6A can slightly reduce RNase H1 cleavage extent over time in test tubes, it could affect RNase H1 activity in cells in different sequence or structural contexts. The m6A modification is known to affect RNA structure and, in turn, affect RNA binding protein accessibility.[40,41] Moreover, the effects of the m6A modification are commonly propagated through the activity of reader proteins, suggesting that m6A sites are often bound by proteins, and, therefore, may generally be inaccessible to PS-ASOs, as we observed for the *MAT2A* stem loop (data not shown). Therefore, as with the other tested modifications, we believe m6A sites in RNA should be avoided during PS-ASO target selection.

Our results are consistent with what is known about how PS-ASOs mediate RNase H1 cleavage of RNA and elucidate the effects of common RNA modifications on enzymatic activity. In general, RNA modifications tend to reduce activity and different modifications, depending on where they are placed on the nucleotide, can affect RNase

H1 activity through different mechanisms and to varying extents. Some modifications may affect RNase H1 cleavage in a sequence-dependent manner, though for other modifications we observe a consistent effect in different sequences. Overall, our work suggests that RNA modifications can affect PS-ASO activity, and should be avoided during target selection, which should be feasible given the extensive information on modification locations within the transcriptome.[47,94]

MATERIALS AND METHODS

Reagents
PS-ASOs and stem-loop RNAs used in this study are listed in the supplemental information (Tables S1 and S2). The chemistries of the gapmer PS-ASOs were either 5-10-5 MOE or 3-10-3 cEt and are color coded in the table. Primer probe sets used in quantitative reverse-transcriptase PCR (qRT-PCR) and those used to sequence the *GINS1* 3'UTR are listed in Table S3.

All synthesized RNAs used in this study were purchased from IDT and resolved on a 12% PAGE gel to remove contaminants and degraded RNA fragments. After gel extraction, the RNAs were ethanol precipitated and reconstituted in water for use in cleavage assays.

Expression and purification of human RNase H1 protein was previously described.[91]

RNase H1 cleavage assays
All cleavage assays were performed under multiple turnover conditions where the substrate duplex concentration was 200 nM and the enzyme concentration was 2.3 nM. RNAs were P32 labeled by PNK and excess ATP was removed by spin column (Cytiva). Labeled and unlabeled RNA were mixed at roughly a 1:8 ratio.

For the size-matched RNA/PS-ASO cleavage assays, duplexes were formed by heating the RNA and PS-ASO at a 1.1:1 ratio at 95°C for 2 min followed by slow cooling at room temperature for 1 h in reaction buffer containing 20 mM Tris 7.5, 50 mM NaCl, 2 mM MgCl$_2$, and 10 mM DTT. For the stem-loop RNA cleavage assays, the RNA first was refolded by heating at 95°C for 2 min then slow cooling at room temperature for 1 h, before the addition of the PS-ASO (1.1:1 molar ratio RNA:PS-ASO) at 37°C for an additional 30 min.

Recombinant, full-length RNase H1 was renatured in the same buffer at room temperature for 1 h. The enzyme was added to the duplex and the reaction proceeded at 37°C for 10 min. For time courses, aliquots were removed at the designated time points. To stop the reaction, an equal volume of RNA loading dye (95% formamide, 18 mM EDTA) was added and the reaction was boiled at 95°C for 2 min before loading onto the gel. Gels were dried and exposed to phosphor screen for visualization. ImageQuant was used to define lanes, subtract background signal, and quantify band intensities. The fraction cleaved is defined as the sum of the product bands relative to the total intensity of the substrate and product bands. The product signal at

0 min was subtracted from the product signal at subsequent time points to demonstrate the accumulated cleavage products over time. Each point is the average of three replicates, with error bars representing SD.

T$_m$ measurements
Duplexes were formed as described above in the RNase H1 cleavage assays at a 4-μM concentration in buffer containing 100 mM NaCl, 10 mM phosphate, and 10 mM EDTA pH 7. Thermal denaturation temperatures (T$_m$ values) were measured in quartz cuvettes (path-length 1.0 cm) on a Cary 100-UV visible spectrophotometer equipped with a Peltier temperature controller. Absorbance at 260 nm was measured as a function of temperature using a temperature ramp of 0.5°C per min. T$_m$ values were determined using the derivative method incorporated into the instrument software. Bar represents the average of three replicates with error bars showing the standard error of the mean.

Cell culture and ADAR1 overexpression cell line
HEK 293 or 293FT cells (ATCC) were cultured at 37°C, with 5% CO$_2$, in DMEM medium supplemented with 10% fetal bovine serum, 0.1 μg/mL streptomycin, and 100 units/mL penicillin.

To generate the stable cell line overexpressing ADAR1, 1 μg plasmid (Origene #RC207522) was transfected into HEK 293 cells and a stable cell line was selected by passaging cells in the presence of 0.5 mg/mL Geneticin (Thermo Fisher).

siRNA treatment
Two siRNAs targeting ADAR1 (Assay Id: 119,580 and 119,581; Thermo Fisher) were transfected at 10 nM total concentration using Lipofectamine RNAiMAX (Life Technologies) at 6 μL of transfection reagent/mL of media; 48 h later, cells were reseeded into a 96-well plate for subsequent studies, or cells were collected for western analysis.

PS-ASO transfection
PS-ASOs were transfected using Lipofectamine 2000 at 4 μL of transfection reagent/mL of media. For reduction of *SNORD8*, cells were transfected with 10 nM of PS-ASOs targeting *SNORD8* or a length- and chemistry-matched control PS-ASO for 72 h and reseeded in a 96-well plate. For PS-ASO activity assays, cells were transfected with titrations of PS-ASOs indicated in the figures and harvested after 5 h (U6) or O/N (*GINS1*).

RNA preparation and qRT-PCR analyses
Total RNA was prepared using a RNeasy mini kit (Qiagen) from cells grown in 96-well plates using the manufacturer's protocol. qRT-PCR was performed in triplicate or quadruplicate using TaqMan primer probe sets as described previously.[95] Briefly, approximately 50 ng total RNA in 5 μL water was mixed with 0.3 μL primer probe sets containing forward and reverse primers (10 μM of each) and fluorescently labeled probe (3 μM), 0.5 μL RT enzyme mix (Qiagen), 4.2 μL RNase-free water, and 10 μL of 2× PCR reaction buffer in a 20 μL

reaction. Reverse transcription was performed at 50°C for 15 min, followed by 95°C for 2 min, and then 40 cycles of PCR were conducted at 95°C for 15 s, and 60°C for 25 s within each cycle using the StepOne Plus RT-PCR system (Applied Biosystems). The mRNA levels were normalized to the amount of total RNA present in each reaction as determined for RNA samples using the Ribogreen assay (Life Technologies). Half maximal inhibitory concentration (IC50) values were calculated using Prism (GraphPad) with the three parameter log[inhibitor] versus response model.

RT-PCR and sequencing of GINS1 3′UTR to detect A-to-I editing

Total RNA was prepared using the RNeasy mini kit (Qiagen) from control and ADAR1 reduced or overexpressing cells; 1 μg of total RNA was added to a Superscript II RT reaction using Random Decamers (Sigma) and following the manufacturer's protocol. Ten microliters of the RT reaction was used as a template in a PCR reaction with the primers listed in Table S3 using cycle parameters 95°C for 30 s, 53°C for 30 s, and 72°C for 60 s, for 40 cycles. PCR products were purified using the PCR clean up kit (Qiagen) and sent for sequencing (Azenta/Genewiz) with the primer listed in Table S3.

Western analysis

Cell pellets were lysed by incubation at 4°C for 10 min in IP Lysis buffer (Pierce). Proteins were collected by centrifugation. Approximately 40 μg protein was separated on 6% to 12% NuPAGE Bis-Tris gradient SDS-PAGE gels (Life Technologies), and transferred onto PVDF membranes using the iBLOT transfer system (Life Technologies). The membranes were blocked with 5% non-fat dry milk in 1×PBS-T at room temperature for 30 min. Membranes were then incubated with primary antibodies (ADAR1-ab126745; GAPDH-Santa Cruz 32,233) at a 1:1,000 dilution at room temperature for 2 h. After three washes with 1×PBS-T, the membranes were incubated with appropriate horseradish peroxidase (HRP)-conjugated secondary antibodies (Bio-Rad 1706515 or 1706516) at room temperature for 1 h to develop the image using Immobilon Forte Western HRP Substrate (Millipore).

Northern blot analysis

Total RNA was isolated from control or SNORD8 ASO-treated cells using Trizol (Life Technologies) according to the manufacturer's protocol. Five micrograms of total RNA was separated on an 8% PAGE gel and semi-dry transferred to Hybond-N+ (Amersham, Arlington Heights, IL) followed by UV cross-linking. After 30 min pre-hybridization in Rapid-Hyb buffer (GE HealthCare) at 42°C, hybridization was performed by incubating the 32 P-labeled DNA oligonucleotide probe in the same buffer at 42°C O/N. Membranes were washed three times with 2x SSC/0.1% SDS at 42°C, for 20 min each time. Hybridization was determined by autoradiography with Phosphor-Imager Storm 860 (Molecular Dynamics, Sunnyvale, CA). The oligonucleotide probes used for northern blots were 5′-TGTTAAACTCACTG GCACCC-3′ for SNORD8, 5′-TGGAACGCTTCACGAATTTGC G-3′ for U6 snRNA, and 5′-CTCAGCCTCCCGAGTAGCTG-3′ for the 7SL control.

DMS footprinting

293FT control or ADAR1 overexpressing cells were grown in two 15-cm dishes. One dish of each condition was treated with 300 μL DMS (Sigma) for 3 min at 37°C. Medium was removed and cells were washed with 30% BME in PBS, then PBS two times. Control dishes were washed with 30% BME and PBS twice. Total RNA was prepared using Trizol according to the manufacturer's protocol. Samples were analyzed by primer extension: total RNA and P32-labeled primer 5′-CTCCTGAGCTCAAGTGATCC-3′ were added to a Superscript II reverse transcription reaction according to the manufacturer's protocol. DNA sequencing was done using the Sequenase 2.0 kit (Applied Biosystems) with a PCR product of the region of interest in the GINS1 3′UTR as a template. The completed RT and DNA sequencing reactions were resolved on a 6% PAGE 0.4 mm gel to identify the inosine-modified nucleotide (Figure S5B).

Primer extension for 2′OMe identification

Total RNA from control and SNORD8 ASO-treated cells was prepared using Trizol according to the manufacturer's protocol. Reverse transcription reactions were carried out using primer 5′-CGTGTCAT CCTTGCGCAGGG-3′ as described above except duplicate reactions were prepared with 0.02 mM dNTPs. Samples were resolved on 6% PAGE 0.4 mm gel and the modified nucleotides were identified as differential primer extension stops between the low and high dNTP reactions and by counting from the excess primer band on the gel (Figure S3B). The intensity of these bands was quantified between control and SNORD8 reduced conditions and the average of three replicates is shown relative to the intensity of the band in the control condition in the bar graph.

AUTHOR CONTRIBUTIONS

K.D.L., X.H.L., and S.T.C. designed the study and wrote the paper. K.D.L. performed the experiments. L.Z. purified the RNase H1 enzyme. All authors analyzed the data.

DECLARATION OF INTERESTS

All authors are current or previous employees of Ionis Pharmaceuticals.

REFERENCES

1. Nguyen, H.D., Yadav, T., Giri, S., Saez, B., Graubert, T.A., and Zou, L. (2017). Functions of replication protein A as a sensor of R loops and a regulator of RNaseH1. Mol. Cell 65, 832–847.e4. https://doi.org/10.1016/j.molcel.2017.01.029.

2. Liang, X-h, Sun, H., Shen, W., and Crooke, S.T. (2015). Identification and characterization of intracellular proteins that bind oligonucleotides with phosphorothioate linkages. Nucleic Acids Res. 43, 2927–2945. https://doi.org/10.1093/nar/gkv143.

3. Vickers, T.A., Rahdar, M., Prakash, T.P., and Crooke, S.T. (2019). Kinetic and subcellular analysis of PS-ASO/protein interactions with P54nrb and RNase H1. Nucleic Acids Res. *47*, 10865–10880. https://doi.org/10.1093/nar/gkz771.

4. Wu, H., Sun, H., Liang, X., Lima, W.F., and Crooke, S.T. (2013). Human RNase H1 is associated with protein P32 and is involved in mitochondrial pre-rRNA processing. PLoS One *8*, e71006. https://doi.org/10.1371/journal.pone.0071006.

5. Lima, W.F., Vickers, T.A., Nichols, J., Li, C., and Crooke, S.T. (2014). Defining the factors that contribute to on-target specificity of antisense oligonucleotides. PLoS One *9*, e101752. https://doi.org/10.1371/journal.pone.0101752.

6. Wan, W.B., and Seth, P.P. (2016). The medicinal chemistry of therapeutic oligonucleotides. J. Med. Chem. *59*, 9645–9667. https://doi.org/10.1021/acs.jmedchem.6b00551.

7. Kurreck, J. (2003). Antisense technologies. Improvement through novel chemical modifications. Eur. J. Biochem. *270*, 1628–1644. https://doi.org/10.1046/j.1432-1033.2003.03555.x.

8. Vickers, T.A., and Crooke, S.T. (2015). The rates of the major steps in the molecular mechanism of RNase H1-dependent antisense oligonucleotide induced degradation of RNA. Nucleic Acids Res. *43*, 8955–8963. https://doi.org/10.1093/nar/gkv920.

9. Vickers, T.A., and Crooke, S.T. (2014). Antisense oligonucleotides capable of promoting specific target mRNA reduction via competing RNase H1-dependent and independent mechanisms. PLoS One *9*, e108625. https://doi.org/10.1371/journal.pone.0108625.

10. Hodges, D., and Crooke, S.T. (1995). Inhibition of splicing of wild-type and mutated luciferase-adenovirus pre-mRNAs by antisense oligonucleotides. Mol. Pharmacol. *48*, 905–918.

11. Liang, X.-H., Sun, H., Nichols, J.G., and Crooke, S.T. (2017). RNase H1-dependent antisense oligonucleotides are robustly active in directing RNA cleavage in both the cytoplasm and the nucleus. Mol. Ther. *25*, 2075–2092. https://doi.org/10.1016/j.ymthe.2017.06.002.

12. Liang, X-h, Sun, H., Shen, W., Wang, S., Yao, J., Migawa, M.T., Bui, H.-H., Damle, S.S., Riney, S., Graham, M.J., et al. (2017). Antisense oligonucleotides targeting translation inhibitory elements in 5′ UTRs can selectively increase protein levels. Nucleic Acids Res. *45*, 9528–9546. https://doi.org/10.1093/nar/gkx632.

13. Liang, X-h, Nichols, J.G., De Hoyos, C.L., and Crooke, S.T. (2020). Some ASOs that bind in the coding region of mRNAs and induce RNase H1 cleavage can cause increases in the pre-mRNAs that may blunt total activity. Nucleic Acids Res. *48*, 9840–9858. https://doi.org/10.1093/nar/gkaa715.

14. Crooke, S.T., Baker, B.F., Crooke, R.M., and Liang, X-h (2021). Antisense technology: an overview and prospectus. Nat. Rev. Drug Discov. *20*, 427–453. https://doi.org/10.1038/s41573-021-00162-z.

15. Crooke, S.T., Liang, X-h, Baker, B.F., and Crooke, R.M. (2021). Antisense technology: a review. J. Biol. Chem. *296*, 100416. https://doi.org/10.1016/j.jbc.2021.100416.

16. Crooke, S.T., Liang, X-h, Crooke, R.M., Baker, B.F., and Geary, R.S. (2021). Antisense drug discovery and development technology considered in a pharmacological context. Biochem. Pharmacol. *189*, 114196. https://doi.org/10.1016/j.bcp.2020.114196.

17. Crooke, S.T., Seth, P.P., Vickers, T.A., and Liang, X-h (2020). The interaction of phosphorothioate-containing RNA targeted drugs with proteins is a critical determinant of the therapeutic effects of these agents. J. Am. Chem. Soc. *142*, 14754–14771. https://doi.org/10.1021/jacs.0c04928.

18. Adachi, H., Hengesbach, M., Yu, Y.-T., and Morais, P. (2021). From antisense RNA to RNA modification: therapeutic potential of RNA-based technologies. Biomed *9*, 550. https://doi.org/10.3390/biomedicines9050550.

19. Lim, K.R.Q., and Yokota, T. (2020). Invention and early history of gapmers. Methods Mol. Biol. *2176*, 3–19. https://doi.org/10.1007/978-1-0716-0771-8_1.

20. Lesnik, E.A., Guinosso, C.J., Kawasaki, A.M., Sasmor, H., Zounes, M., Cummins, L.L., Ecker, D.J., Cook, P.D., and Freier, S.M. (1993). Oligodeoxynucleotides containing 2'-O-modified adenosine: synthesis and effects on stability of DNA:RNA duplexes. Biochemistry *32*, 7832–7838. https://doi.org/10.1021/bi00081a031.

21. Prakash, T.P. (2011). An overview of sugar modified oligonucleotides for antisense therapeutics. Chem. Biodivers. *8*, 1616–1641. https://doi.org/10.1002/cbdv.201100081.

22. Egli, M., Minasov, G., Tereshko, V., Pallan, P.S., Teplova, M., Inamati, G.B., Lesnik, E.A., Owens, S.R., Ross, B.S., Prakash, T.P., and Manoharan, M. (2005). Probing the influence of stereoelectronic effects on the biophysical properties of oligonucleotides: comprehensive analysis of the RNA affinity, nuclease resistance, and crystal structure of ten 2'-O-ribonucleic acid modifications. Biochemistry *44*, 9045–9057. https://doi.org/10.1021/bi050574m.

23. Seth, P.P., Siwkowski, A., Allerson, C.R., Vasquez, G., Lee, S., Prakash, T.P., Kinberger, G., Migawa, M.T., Gaus, H., Bhat, B., and Swayze, E.E. (2008). Design, synthesis and evaluation of constrained methoxyethyl (cMOE) and constrained ethyl (cEt) Nucleoside Analogs. Nucl. Acid S *52*, 553–554. https://doi.org/10.1093/nass/nrn280.

24. Swayze, E.E., Siwkowski, A.M., Wancewicz, E.V., Migawa, M.T., Wyrzykiewicz, T.K., Hung, G., Monia, B.P., and Bennett, a C.F. (2007). Antisense oligonucleotides containing locked nucleic acid improve potency but cause significant hepatotoxicity in animals. Nucleic Acids Res. *35*, 687–700. https://doi.org/10.1093/nar/gkl1071.

25. Kuespert, S., Heydn, R., Peters, S., Wirkert, E., Meyer, A.-L., Siebörger, M., Johannesen, S., Aigner, L., Bogdahn, U., and Bruun, T.-H. (2020). Antisense oligonucleotide in LNA-gapmer design targeting TGFBR2—a key single gene target for safe and effective inhibition of TGFβ signaling. Int. J. Mol. Sci. *21*, 1952. https://doi.org/10.3390/ijms21061952.

26. Kumar, S., Mapa, K., and Maiti, S. (2014). Understanding the effect of locked nucleic acid and 2'- O -methyl modification on the hybridization thermodynamics of a miRNA–mRNA pair in the presence and absence of AfPiwi protein. Biochemistry *53*, 1607–1615. https://doi.org/10.1021/bi401677d.

27. Khvorova, A., and Watts, J.K. (2017). The chemical evolution of oligonucleotide therapies of clinical utility. Nat. Biotechnol. *35*, 238–248. https://doi.org/10.1038/nbt.3765.

28. Sands, H., Gorey-Feret, L.J., Cocuzza, A.J., Hobbs, F.W., Chidester, D., and Trainor, G.L. (1994). Biodistribution and metabolism of internally 3H-labeled oligonucleotides. I. Comparison of a phosphodiester and a phosphorothioate. Mol. Pharmacol. *45*, 932–943.

29. Liang, X.-H., Sun, H., Hsu, C.-W., Nichols, J.G., Vickers, T.A., De Hoyos, C.L., and Crooke, S.T. (2020). Golgi-endosome transport mediated by M6PR facilitates release of antisense oligonucleotides from endosomes. Nucleic. Acids. Res. *48*, 1372–1391. https://doi.org/10.1093/nar/gkz1171.

30. Wang, S., Sun, H., Tanowitz, M., Liang, X-h, and Crooke, S.T. (2016). Annexin A2 facilitates endocytic trafficking of antisense oligonucleotides. Nucleic. Acids. Res. *44*. gkw595-7330. https://doi.org/10.1093/nar/gkw595.

31. Eckstein, F. (2014). Phosphorothioates, essential components of therapeutic oligonucleotides. Nucleic. Acid. Ther. *24*, 374–387. https://doi.org/10.1089/nat.2014.0506.

32. Migawa, M.T., Shen, W., Wan, W.B., Vasquez, G., Oestergaard, M.E., Low, A., De Hoyos, C.L., Gupta, R., Murray, S., Tanowitz, M., et al. (2019). Site-specific replacement of phosphorothioate with alkyl phosphonate linkages enhances the therapeutic profile of gapmer ASOs by modulating interactions with cellular proteins. Nucleic. Acids. Res. *47*, 5465–5479. https://doi.org/10.1093/nar/gkz247.

33. Anderson, B.A., Freestone, G.C., Low, A., De-Hoyos, C.L., Drury, W.J., Østergaard, M.E., Migawa, M.T., Fazio, M., Wan, W.B., Berdeja, A., et al. (2021). Towards next generation antisense oligonucleotides: mesylphosphoramidate modification improves therapeutic index and duration of effect of gapmer antisense oligonucleotides. Nucleic. Acids. Res. *49*, 9026–9041. https://doi.org/10.1093/nar/gkab718.

34. Shen, W., De Hoyos, C.L., Migawa, M.T., Vickers, T.A., Sun, H., Low, A., Bell, T.A., Rahdar, M., Mukhopadhyay, S., Hart, C.E., et al. (2019). Chemical modification of PS-ASO therapeutics reduces cellular protein-binding and improves the therapeutic index. Nat. Biotechnol. *37*, 640–650. https://doi.org/10.1038/s41587-019-0106-2.

35. Vasquez, G., Freestone, G.C., Wan, W.B., Low, A., De Hoyos, C.L.,Y.,J., Yu, J., Østergaard, M.E., Liang, X-h, Crooke, S.T., Swayze, E., et al. (2021). Site-specific incorporation of 5′-methyl DNA enhances the therapeutic profile of gapmer ASOs. Nucleic. Acids. Res. *49*, 1828–1839. https://doi.org/10.1093/nar/gkab047.

36. Lima, W.F., Wu, H., Nichols, J.G., Prakash, T.P., Ravikumar, V., and Crooke, S.T. (2003). Human RNase H1 uses one tryptophan and two lysines to position the enzyme at the 3′-DNA/5′-RNA terminus of the heteroduplex substrate. J. Biol. Chem. *278*, 49860–49867. https://doi.org/10.1074/jbc.m306543200.

37. Lima, W.F., Nichols, J.G., Wu, H., Prakash, T.P., Migawa, M.T., Wyrzykiewicz, T.K., Bhat, B., and Crooke, S.T. (2004). Structural requirements at the catalytic site of the heteroduplex substrate for human RNase H1 catalysis. J. Biol. Chem. 279, 36317–36326. https://doi.org/10.1074/jbc.m405035200.

38. Wu, H., Lima, W.F., and Crooke, S.T. (2001). Investigating the structure of human RNase H1 by site-directed mutagenesis. J. Biol. Chem. 276, 23547–23553. https://doi.org/10.1074/jbc.m009676200.

39. Kumar, S., and Mohapatra, T. (2021). Deciphering epitranscriptome: modification of mRNA bases provides a new perspective for post-transcriptional regulation of gene expression. Front. Cell. Developmental. Biol. 9, 628415. https://doi.org/10.3389/fcell.2021.628415.

40. Liu, N., Dai, Q., Zheng, G., He, C., Parisien, M., and Pan, T. (2015). N6-methyladenosine-dependent RNA structural switches regulate RNA–protein interactions. Nature 518, 560–564. https://doi.org/10.1038/nature14234.

41. Zhou, K.I., Parisien, M., Dai, Q., Liu, N., Diatchenko, L., Sachleben, J.R., and Pan, T. (2016). N6-Methyladenosine modification in a long noncoding RNA hairpin predisposes its conformation to protein binding. J. Mol. Biol. 428, 822–833. https://doi.org/10.1016/j.jmb.2015.08.021.

42. Abou Assi, H., Rangadurai, A.K., Shi, H., Liu, B., Clay, M.C., Erharter, K., Kreutz, C., Holley, C.L., and Al-Hashimi, H.M. (2020). 2′- O -Methylation can increase the abundance and lifetime of alternative RNA conformational states. Nucleic. Acids. Res. 48, 12365–12379. https://doi.org/10.1093/nar/gkaa928.

43. Roundtree, I.A., Evans, M.E., Pan, T., and He, C. (2017). Dynamic RNA modifications in gene expression regulation. Cell 169, 1187–1200. https://doi.org/10.1016/j.cell.2017.05.045.

44. Christofi, T., and Zaravinos, A. (2019). RNA editing in the forefront of epitranscriptomics and human health. J. Transl. Med. 17, 319. https://doi.org/10.1186/s12967-019-2071-4.

45. Boo, S.H., and Kim, Y.K. (2020). The emerging role of RNA modifications in the regulation of mRNA stability. Exp. Mol. Med. 52, 400–408. https://doi.org/10.1038/s12276-020-0407-z.

46. Dimitrova, D.G., Teysset, L., and Carré, C. (2019). RNA 2'-O-methylation (nm) modification in human diseases. Genes-basel 10, 117. https://doi.org/10.3390/genes10020117.

47. Boccaletto, P., Machnicka, M.A., Purta, E., Piątkowski, P., Bagiński, B., Wirecki, T.K., de Crécy-Lagard, V., Ross, R., Limbach, P.A., Kotter, A., Helm, M., and Bujnicki, J.M. (2018). MODOMICS: a database of RNA modification pathways. 2017 update. Nucleic. Acids. Res. 46, D303–D307. https://doi.org/10.1093/nar/gkx1030.

48. Knuckles, P., Carl, S.H., Musheev, M., Niehrs, C., Wenger, A., and Bühler, M. (2017). RNA fate determination through cotranscriptional adenosine methylation and microprocessor binding. Nat. Struct. Mol. Biol. 24, 561–569. https://doi.org/10.1038/nsmb.3419.

49. Picardi, E., Manzari, C., Mastropasqua, F., Aiello, I., D'Erchia, A.M., and Pesole, G. (2015). Profiling RNA editing in human tissues: towards the inosinome Atlas. Scientific. Rep. 5, 14941. https://doi.org/10.1038/srep14941.

50. Laurencikiene, J., Källman, A.M., Fong, N., Bentley, D.L., and Öhman, M. (2006). RNA editing and alternative splicing: the importance of co-transcriptional coordination. EMBO Rep. 7, 303–307. https://doi.org/10.1038/sj.embor.7400621.

51. Zhou, K.I., Shi, H., Lyu, R., Wylder, A.C., Matuszek, Ż., Pan, J.N., He, C., Parisien, M., and Pan, T. (2019). Regulation of Co-transcriptional pre-mRNA splicing by m6A through the low-complexity protein hnRNPG. Mol. Cell. 76, 70–81.e9. https://doi.org/10.1016/j.molcel.2019.07.005.

52. Monaco, P.L., Marcel, V., Diaz, J.-J., and Catez, F. (2018). 2′-O-Methylation of ribosomal RNA: towards an epitranscriptomic control of translation? Biomol 8, 106. https://doi.org/10.3390/biom8040106.

53. Krogh, N., Kongsbak-Wismann, M., Geisler, C., and Nielsen, H. (2017). Substoichiometric ribose methylations in spliceosomal snRNAs. Org. Biomol. Chem. 15, 8872–8876. https://doi.org/10.1039/c7ob02317k.

54. Taoka, M., Nobe, Y., Yamaki, Y., Sato, K., Ishikawa, H., Izumikawa, K., Yamauchi, Y., Hirota, K., Nakayama, H., Takahashi, N., and Isobe, T. (2018). Landscape of the complete RNA chemical modifications in the human 80S ribosome. Nucleic. Acids. Res. 46, 9289–9298. https://doi.org/10.1093/nar/gky811.

55. Liang, X-h, Liu, Q., and Fournier, M.J. (2009). Loss of rRNA modifications in the decoding center of the ribosome impairs translation and strongly delays pre-rRNA processing. RNA 15, 1716–1728. https://doi.org/10.1261/rna.1724409.

56. Elliott, B.A., Ho, H.-T., Ranganathan, S.V., Vangaveti, S., Ilkayeva, O., Abou Assi, H., Choi, A.K., Agris, P.F., and Holley, C.L. (2019). Modification of messenger RNA by 2′-O-methylation regulates gene expression in vivo. Nat. Commun. 10, 3401. https://doi.org/10.1038/s41467-019-11375-7.

57. Byszewska, M., Śmietański, M., Purta, E., and Bujnicki, J.M. (2015). RNA methyltransferases involved in 5′ cap biosynthesis. Rna. Biol. 11, 1597–1607. https://doi.org/10.1080/15476286.2015.1004955.

58. Dai, Q., Moshitch-Moshkovitz, S., Han, D., Kol, N., Amariglio, N., Rechavi, G., Dominissini, D., and He, C. (2017). Nm-seq maps 2′-O-methylation sites in human mRNA with base precision. Nat. Methods 14, 695–698. https://doi.org/10.1038/nmeth.4294.

59. Cavaillé, J., Nicoloso, M., and Bachellerie, J.-P. (1996). Targeted ribose methylation of RNA in vivo directed by tailored antisense RNA guides. Nature 383, 732–735. https://doi.org/10.1038/383732a0.

60. Bachellerie, J.-P., and Cavaillé, J. (1997). Guiding ribose methylation of rRNA. Trends Biochem. Sci. 22, 257–261. https://doi.org/10.1016/s0968-0004(97)01057-8.

61. Somme, J., Van Laer, B., Roovers, M., Steyaert, J., Versées, W., and Droogmans, L. (2014). Characterization of two homologous 2′-O-methyltransferases showing different specificities for their tRNA substrates. RNA 20, 1257–1271. https://doi.org/10.1261/rna.044503.114.

62. Peng, Z., Cheng, Y., Tan, B.C.-M., Kang, L., Tian, Z., Zhu, Y., Zhang, W., Liang, Y., Hu, X., Tan, X., et al. (2012). Comprehensive analysis of RNA-Seq data reveals extensive RNA editing in a human transcriptome. Nat. Biotechnol. 30, 253–260. https://doi.org/10.1038/nbt.2122.

63. Ramaswami, G., and Li, J.B. (2014). RADAR: a rigorously annotated database of A-to-I RNA editing. Nucleic. Acids. Res. 42, D109–D113. https://doi.org/10.1093/nar/gkt996.

64. Kim, U., Wang, Y., Sanford, T., Zeng, Y., and Nishikura, K. (1994). Molecular cloning of cDNA for double-stranded RNA adenosine deaminase, a candidate enzyme for nuclear RNA editing. Proc. Natl. Acad. Sci. 91, 11457–11461. https://doi.org/10.1073/pnas.91.24.11457.

65. Lai, F., Chen, C.X., Carter, K.C., and Nishikura, K. (1997). Editing of glutamate receptor B subunit ion channel RNAs by four alternatively spliced DRADA2 double-stranded RNA adenosine deaminases. Mol. Cell. Biol. 17, 2413–2424. https://doi.org/10.1128/mcb.17.5.2413.

66. Nishikura, K., Yoo, C., Kim, U., Murray, J.M., Estes, P.A., Cash, F.E., and Liebhaber, S.A. (1991). Substrate specificity of the dsRNA unwinding/modifying activity. EMBO J. 10, 3523–3532. https://doi.org/10.1002/j.1460-2075.1991.tb04916.x.

67. Wright, D.J., Rice, J.L., Yanker, D.M., and Znosko, B.M. (2007). Nearest neighbor parameters for Inosine·Uridine pairs in RNA duplexes. Biochemistry 46, 4625–4634. https://doi.org/10.1021/bi0616910.

68. Wright, D.J., Force, C.R., and Znosko, B.M. (2018). Stability of RNA duplexes containing inosine·cytosine pairs. Nucleic. Acids. Res. 46, 12099–12108. https://doi.org/10.1093/nar/gky907.

69. Nishikura, K. (2006). Editor meets silencer: crosstalk between RNA editing and RNA interference. Nat. Rev. Mol. Cell. Biol. 7, 919–931. https://doi.org/10.1038/nrm2061.

70. Samuel, C.E. (2019). Adenosine deaminase acting on RNA (ADAR1), a suppressor of double-stranded RNA–triggered innate immune responses. J. Biol. Chem. 294, 1710–1720. https://doi.org/10.1074/jbc.tm118.004166.

71. Rueter, S.M., Dawson, T.R., and Emeson, R.B. (1999). Regulation of alternative splicing by RNA editing. Nature 399, 75–80. https://doi.org/10.1038/19992.

72. Seeburg, P.H., Higuchi, M., and Sprengel, R. (1998). RNA editing of brain glutamate receptor channels: mechanism and physiology1Published on the World Wide Web on 5 February 1998.1. Brain Res. Rev. 26, 217–229. https://doi.org/10.1016/s0165-0173(97)00062-3.

73. Anantharaman, A., Gholamalamdari, O., Khan, A., Yoon, J.-H., Jantsch, M.F., Hartner, J.C., Gorospe, M., Prasanth, S.G., and Prasanth, K.V. (2017). RNA -editing enzymes ADAR 1 and ADAR 2 coordinately regulate the editing and expression of

Ctn <scp>RNA</scp>. FEBS Lett. *591*, 2890–2904. https://doi.org/10.1002/1873-3468.12795.

74. Dominissini, D., Moshitch-Moshkovitz, S., Schwartz, S., Salmon-Divon, M., Ungar, L., Osenberg, S., Cesarkas, K., Jacob-Hirsch, J., Amariglio, N., Kupiec, M., et al. (2012). Topology of the human and mouse m6A RNA methylomes revealed by m6A-seq. Nature *485*, 201–206. https://doi.org/10.1038/nature11112.

75. Meyer, K.D., Saletore, Y., Zumbo, P., Elemento, O., Mason, C.E., and Jaffrey, S.R. (2012). Comprehensive analysis of mRNA methylation reveals enrichment in 3' UTRs and near stop codons. Cell *149*, 1635–1646. https://doi.org/10.1016/j.cell.2012.05.003.

76. Pendleton, K.E., Chen, B., Liu, K., Hunter, O.V., Xie, Y., Tu, B.P., and Conrad, N.K. (2017). The U6 snRNA m6A methyltransferase METTL16 regulates SAM synthetase Intron retention. Cell *169*, 824–835.e14. https://doi.org/10.1016/j.cell.2017.05.003.

77. Spitale, R.C., Flynn, R.A., Zhang, Q.C., Crisalli, P., Lee, B., Jung, J.-W., Kuchelmeister, H.Y., Batista, P.J., Torre, E.A., et al. (2015). Structural imprints in vivo decode RNA regulatory mechanisms. Nature *519*, 486–490. https://doi.org/10.1038/nature14263.

78. Roost, C., Lynch, S.R., Batista, P.J., Qu, K., Chang, H.Y., Kool, et al. (2015). Structure and thermodynamics of N6-methyladenosine in RNA: a spring-loaded base modification. J. Am. Chem. Soc. *137*, 2107–2115. https://doi.org/10.1021/ja513080v.

79. Sun, L., Fazal, F.M., Li, P., Broughton, J.P., Lee, B., Tang, L., Huang, W., Kool, E.T., Chang, H.Y., and Zhang, Q.C. (2019). RNA structure maps across mammalian cellular compartments. Nat. Struct. Mol. Biol. *26*, 322–330. https://doi.org/10.1038/s41594-019-0200-7.

80. Kierzek, E., and Kierzek, R. (2003). The thermodynamic stability of RNA duplexes and hairpins containing N6 alkyladenosines and 2 methylthio N6 alkyladenosines. Nucleic Acids Res. *31*, 4472–4480. https://doi.org/10.1093/nar/gkg633.

81. Kierzek, E., Zhang, X., Watson, R.M., Kennedy, S.D., Szabat, M., Kierzek, R., and Mathews, D.H. (2022). Secondary structure prediction for RNA sequences including N6-methyladenosine. Nat. Commun. *13*, 1271. https://doi.org/10.1038/s41467-022-28817-4.

82. Zaccara, S., Ries, R.J., and Jaffrey, S.R. (2019). Reading, writing and erasing mRNA methylation. Nat. Rev. Mol. Cell. Biol. *20*, 608–624. https://doi.org/10.1038/s41580-019-0168-5.

83. Nowotny, M., Gaidamakov, S.A., Ghirlando, R., Cerritelli, S.M., Crouch, R.J., and Yang, W. (2007). Structure of human RNase H1 complexed with an RNA/DNA hybrid: Insight into HIV reverse transcription. Mol. Cell. *28*, 264–276. https://doi.org/10.1016/j.molcel.2007.10.021.

84. Freier, S.M., and Altmann, K.H. (1997). The ups and downs of nucleic acid duplex stability: structure-stability studies on chemically-modified DNA:RNA duplexes. Nucleic. Acids. Res. *25*, 4429–4443. https://doi.org/10.1093/nar/25.22.4429.

85. Parker, B.J., Moltke, I., Roth, A., Washietl, S., Wen, J., Kellis, M., Breaker, R., and Pedersen, J.S. (2011). New families of human regulatory RNA structures identified by comparative analysis of vertebrate genomes. Genome. Res. *21*, 1929–1943. https://doi.org/10.1101/gr.112516.110.

86. Ganot, P., Jády, B.E., Bortolin, M.-L., Darzacq, X., and Kiss, T. (1999). Nucleolar factors direct the 2′-O-ribose methylation and pseudouridylation of U6 spliceosomal RNA. Mol. Cell. Biol. *19*, 6906–6917. https://doi.org/10.1128/mcb.19.10.6906.

87. Yu, Y.T., Shu, M.D., and Steitz, J.A. (1997). A New Method for Detecting Sites of 2'-O-Methylation in RNA Molecules. RNA *3*, 324–331.

88. Fury, M.G., and Zieve, G.W. (1996). U6 snRNA maturation and stability. Exp. Cell. Res. *228*, 160–163. https://doi.org/10.1006/excr.1996.0311.

89. Brümmer, A., Yang, Y., Chan, T.W., and Xiao, X. (2017). Structure-mediated modulation of mRNA abundance by A-to-I editing. Nat. Commun. *8*, 1255. https://doi.org/10.1038/s41467-017-01459-7.

90. Strehblow, A., Hallegger, M., and Jantsch, M.F. (2002). Nucleocytoplasmic distribution of human RNA-editing enzyme ADAR1 is modulated by double-stranded RNA-binding domains, a leucine-rich export signal, and a putative dimerization domain. Mol. Biol. Cell. *13*, 3822–3835. https://doi.org/10.1091/mbc.e02-03-0161.

91. Zhang, L., Vickers, T.A., Sun, H., Liang, X-h, and Crooke, S.T. (2021). Binding of phosphorothioate oligonucleotides with RNase H1 can cause conformational changes in the protein and alter the interactions of RNase H1 with other proteins. Nucleic. Acids. Res. *49*, 2721–2739. https://doi.org/10.1093/nar/gkab078.

92. Nowotny, M., Gaidamakov, S.A., Crouch, R.J., and Yang, W. (2005). Crystal structures of RNase H bound to an RNA/DNA hybrid: substrate specificity and metal-dependent catalysis. Cell *121*, 1005–1016. https://doi.org/10.1016/j.cell.2005.04.024.

93. Maranon, D.G., and Wilusz, J. (2020). Mind the gapmer: implications of co-transcriptional cleavage by antisense oligonucleotides. Mol. Cell. *77*, 932–933. https://doi.org/10.1016/j.molcel.2020.02.010.

94. Picardi, E., D'Erchia, A.M., Lo Giudice, C., and Pesole, G. (2017). REDIportal: a comprehensive database of A-to-I RNA editing events in humans. Nucleic. Acids. Res. *45*, D750–D757. https://doi.org/10.1093/nar/gkw767.

95. Liang, X-h, Hart, C.E., and Crooke, S.T. (2013). Transfection of siRNAs can alter miRNA levels and trigger non-specific protein degradation in mammalian cells. Biochim. Biophys. Acta (Bba) - Gene Regul. Mech. *1829*, 455–468. https://doi.org/10.1016/j.bbagrm.2013.01.011.